

***In Vitro* Flow Study in an Intracranial Aneurysm Biomodel Manufactured by Additive Manufacturing**

Andrews Souza^{1,2,3}^a, Diana Rodrigues¹, Maria Sabrina Souza⁴^b, Conrado Ferrera⁵^c, João Ribeiro^{3,4}^d, Rui A. Lima^{1,2}^e and Ana Moita^{6,7}^f

¹University of Minho, Campus de Azurém, 4800-058 Guimarães, Portugal

²Mechanical Engineering and Resource Sustainability Center (MEtRICs), UMinho, Guimarães, Portugal

³Centro de Investigação de Montanha (CIMO), Instituto Politécnico de Bragança (IPB),
Campus de Santa Apolónia, 5300-253 Bragança, Portugal

⁴Instituto Politécnico de Bragança, 5300-253, Bragança, Portugal

⁵Depto. de Ingeniería Mecánica, Energética y de los Materiales and Instituto de Computación Científica Avanzada,
Universidad de Extremadura, Badajoz, Spain

⁶IN+, Center for Innovation, Technology and Policy Research, Instituto Superior Técnico,
Universidade de Lisboa, Av. Rovisco Pais, 1049-001 Lisboa, Portugal

⁷CINAMIL, Department of Exact Sciences and Engineering, Portuguese Military Academy,
R. Gomes Freire 203, 1169-203 Lisboa, Portugal

Keywords: Aneurysm Intracranial Biomodels, *in Vitro* Tests, Additive Manufacturing, Polysmooth.

Abstract: The hemodynamics of Intracranial Aneurysm (IA) involves complex phenomena that influence its growth and rupture. The progress of additive manufacturing techniques has allowed the development of biomodels suitable to perform *in vitro* flow experiments. Hence, this work presents the manufacturing process to fabricate flow biomodels by using the additive manufacturing technique known as Fused Deposition Modeling (FDM). The biomodels obtained through the proposed technique has proved to be suitable for *in vitro* flow experiments using imaging techniques and for validation of numerical studies.

1 INTRODUCTION

Intracranial Aneurysm (IA) is a disease associated with weakening of the arterial wall, which causes local dilation (Rodríguez-Régent et al., 2014). This pathology has a high mortality rate of around 60% after rupture (Amenta et al., 2012). Studies have shown that changes in flow induce endothelial cell responses, thus causing disease (Chiu & Chien, 2011), but the cause of development and disruption of IAs are still not well understood (Tromp et al., 2014). Therefore, to better understand IAs, it is important to analyze the local hemodynamic, and how it affects the vessel wall (Saqr et al., 2019).

Although there are non-invasive *in vivo* studies capable of performing flow measurements using

imaging techniques such as Phase Contrast Magnetic Resonance Imaging (PC-MRI), Magnetic Resonance Angiography (MRA), these have difficulty in visualizing the flow due to lack of resolution in small vessels only underestimate wall shear values, have low reproducibility and are expensive (Szajer & Ho-Shon, 2018)(Rolloff et al., 2018).

As an alternative to *in vivo* studies, *in vitro* tests with transparent flow phantoms (biomodels) make it possible to visualize the flow through the monitoring of suspended tracer particles. It is possible to employ different techniques for measurement, such as Particle Image Velocimetry (PIV) (Yamaguchi et al., 2022), Particle Tracking Velocimetry (PTV) and image microscopy (Souza et al., 2020). Another advantage of *in vitro* studies is the possibility of

^a <https://orcid.org/0000-0003-2414-073X>

^b <https://orcid.org/0000-0002-4415-7267>

^c <https://orcid.org/0000-0002-2274-1374>

^d <https://orcid.org/0000-0001-6300-148X>

^e <https://orcid.org/0000-0003-3428-637X>

^f <https://orcid.org/0000-0001-9801-7617>

validating numerical simulations. The disadvantage of this type of study is the difficulty of manufacturing biomodels suitable for tests, as these flow phantoms must be transparent, they must reproduce the anatomical geometry, and the lost core material must not interact with the biomodel material. In recent years, the aid of Additive Manufacturing (AM) techniques has enabled the proper fabrication of IA biomodels. Souza et al (Souza et al., 2020) combined AM processes and lost core casting with glycerin-based soap, and Doutel et al (Doutel et al., 2015) used caramel (melted sugar) as the lost core material. Although these processes have been shown to be adequate, they have many steps in their manufacture.

In this work, a biomodel manufacturing process is presented, which uses AM techniques to directly print the model of the lost core (vessel lumen), which is coated with a transparent, biocompatible silicone, which is Polydimethylsiloxane (PDMS). One of the advantages of this silicone is its ease of manufacture, when compared to models made of glass (Yu & Durgesh, 2022). The biomodels were tested for their transparency and high-speed video microscopy tests were performed for qualitative analysis of flow behavior and quantitative analysis of flow velocity.

2 BIOMODEL MANUFACTURING PROCESS

The geometry used was previously created in the SolidWorks 3D CAD Software, using the average dimensions of real intracranial aneurysms (Parlea et al., 1999). The geometry was saved in STL format and then converted to G-code, a format used in 3D printers. The spherical geometry was chosen, because according to the study by (Philip et al., 2022) that compares through numerical studies the idealized and patient-specific geometries that the physics of the flow inside the aneurysm sac is better predicted in this type of geometry.

The Biomodels were manufactured using an additive manufacturing technique, Fused Deposition Modeling (FDM). The geometry was printed in PolySmooth (chosen material) in the Ultimaker 3 3D printer. After obtaining the model, it was positioned in the Polysher machine for a surface treatment with isopropyl alcohol, this treatment took place for a period of 20 minutes, way that the lines of the outermost layers of geometry are smoothed. With the surface treatment completed, the mold was placed in an acetate box and then the PDMS was poured by gravity. PDMS was prepared in a ratio of 10:1 and its

curing process took place in 48 hours. After the PDMS had completely cured, the lost core material was removed with isopropyl alcohol. The process steps are illustrated in Figure 1.

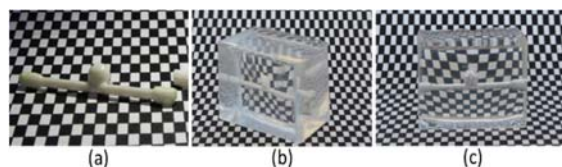


Figure 1: (a) PolySmooth geometry, (b) biomodel with lost core material and (c) final biomodel.

3 EVALUATION OF THE OPTICAL TRANSPARENCY OF THE BIOMODEL

To evaluate the issue of optical distortion caused by solid-liquid interaction, two fluids with different physical properties were tested. At first, a fluid with a refractive index similar to that of PDMS and was used, a mixture of 61% glycerol and 39% distilled water (w/w) and 0.06% suspended particles of Polymethylmethacrylate (PMMA) with 60 μm (in diameter). The second fluid considered was just water. It is important to mention that the application of this technique, to evaluate the optical transparency of the biomodel under study, was based on the work carried out by Hopkins et al (Hopkins et al., 2000). The physical properties of the materials used in the present study are shown in Table 1 (Souza et al., 2020).

Table 1: Physical properties of materials used in the evaluation of the optical transparency of biomodels.

Material	Refractive index	Viscosity (Pa.s)	Density (kg/m ³)
Water	1.333	0.920×10^{-3}	997
Glycerin mixture	1.412	1.290×10^{-2}	1153
PDMS	1.412	-	-

In the tests, a sheet with a rectangular structure was used in which each rectangle has dimensions of 2.4 × 3.9 mm and under which the biomodel was placed with the different fluids. Figure 2 shows the images of the transparency tests, with image (a) referring to the biomodel in which the injected fluid was water and image (b) corresponding to the situation in which the glycerin-based solution was injected.



Figure 2: Evaluation of the optical transparency of the biomodel with the fluid: (a) water and (b) glycerin-based solution.

4 EXPERIMENTAL TEST OF FLOW VISUALIZATION

The main objectives of this test were: to evaluate the appearance of the fluid recirculation phenomenon as a function of the flow rates used, through the observation of the particle trajectories and; evaluate the velocities in different zones of the biomodel.

For this, an experimental setup was used, consisting of a set of equipment, namely: an ultra-high-speed camera (Photron FASTCAM SA3), coupled to an inverted microscope (IX71, Olympus, Japan) and an objective (N-Achroplan 2.5x/0.07). At first, the PDMS biomodel was fixed to the microscope and a syringe pump was used to pump the working fluid at a constant flow rate. Two different flow rates were used: 5 ml/min and 20 ml/min.

4.1 Qualitative Analysis of Flow Behavior

The recorded images, using the Photron FASTCAM visualization software, were later processed in the ImageJ software, where the particle trajectories and velocities were obtained using the Z Project plugin and the MTrackJ plugin, respectively. The image processing of the two flows studied are shown in Figure 3.

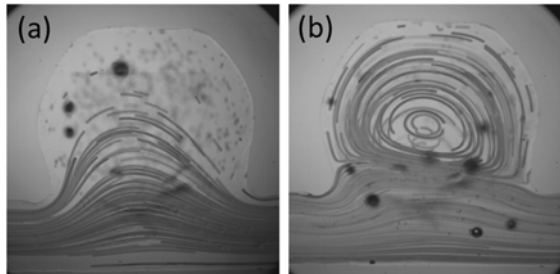


Figure 3: Trajectories of the PMMA particles for a flow rate of: (a) 5 ml/min and (b) 20 ml/min.

Observing the previous figure, it can be concluded that, for a flow rate of 5 mL/min, the phenomenon of fluid recirculation still does not occur. However, it is possible to verify that for the flow of 20 mL/min, the phenomenon of fluid recirculation occurs. Although the flow rates used are lower than those found in cerebral arteries, the technique demonstrates the potential of observing the different phenomena that occur within IAs with an increase in the flow rate. Thus, characterizing and visualizing the vortex zones, which is a characteristic related to IAs growth and rupture (Saqr et al., 2019).

4.2 Quantitative Analysis of Flow Velocity

To study the velocities, the images were processed with the ImageJ software with the MTrackJ plugin. Velocity was evaluated in 5 zones: at the inlet, at the outlet and at three locations in the center of the biomodel, for both flows. Figure 4 shows the trajectories where the velocities for the different flow rates were obtained.

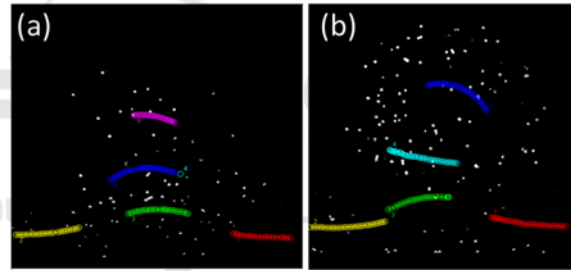


Figure 4: Trajectory of the marked particles, for the flow rate of (a) 5ml/min and (b) 20 ml/min.

With the trajectories traced, it was then possible to calculate the velocities in each of the marked areas. Therefore, the results obtained for the velocity in the study with flow rate of 5 ml/min are found in Table 2 and Table 3 shows the results for the flow rate of 20 ml/min.

Table 2: Velocities obtained considering a flow rate of 5 ml/min.

Track			Velocity m/s
1	Red	Inlet	0.0120
2	Yellow	Outlet	0.0156
3	Light green	Center	0.0061
4	Dark blue	Center	0.0040
5	Pink	Center	0.0008

Table 3: Velocities obtained considering a flow rate of 20 ml/min.

Track			Velocity m/s
1	Red	Inlet	0.0595
2	Yellow	Outlet	0.0659
3	Light green	Center	0.0327
4	Light blue	Center	0.0137
5	Dark blue	Center	0.0039

With the velocity profiles traced, we observed that the velocities of the fluid inside the aneurysm sac for both studied flow rates are lower than the inlet and outlet flows. At the flow rate of 20 ml/min where recirculation occurs, the flow velocity decreases even more as it approaches the upper part of the aneurysm head. Although the flow rates used in our tests are lower than the real values, the behavior of the velocities found corresponds to previous studies (Philip et al., 2022)(Cebal et al., 2011), where the velocity decreases in the vortex zones.

5 CONCLUSIONS

Intracranial aneurysms are severe diseases that require deeper understanding for a better diagnosis and treatment of this kind of pathology. *In vitro* hemodynamic studies are a promising way to improve our understanding about the beginning, development, and rupture of intracranial aneurysms. The obtained experimental flow results have shown that the polysmooth material that was used by FDM printing technique was proved to be suitable for the manufacture of biomodels, with good dimensional accuracy, high quality flow visualizations and ease to remove the material from the lumen. Through the visualization tests, it was possible to identify the recirculation regions at the highest flow. In addition, it was possible to observe that at the central region of the aneurysm, where the recirculation occurs, the velocities are much lower when compared to the inlet and outlet velocities.

For future work, it is intended to use fluids with rheological properties closer to blood (blood analogues), but with the same refractive index as PDMS. In addition to using flow rates obtained from medical examinations for a more realistic approach.

ACKNOWLEDGEMENTS

The authors acknowledge the financial support provided by Fundação para a Ciência e a Tecnologia

(FCT), through the projects EXPL/EME-EME/0732/2021, PTDC/EEI-EEE/2846/2021, funded by NORTE 2020, PORTUGAL2020, and FEDER. This work was also supported by Fundação para a Ciência e a Tecnologia (FCT) under the strategic grants UIDB/04077/2020, UIDB/00690/2020, UIDB/04436/2020 and UIDB/00532/2020. Andrews Souza acknowledges the PhD scholarship 2021.07961.BD attributed by FCT. Partial support from the Junta de Extremadura through Grants No. GR21091 and IB20105 (partially financed by FEDER funds) is gratefully acknowledged.

REFERENCES

- Amenta, P. S., Yadla, S., Campbell, P. G., Maltenfort, M. G., Dey, S., Ghosh, S., Ali, M. S., Jallo, J. I., Tjoumakaris, S. I., Gonzalez, L. F., Dumont, A. S., Rosenwasser, R. H., & Jabbour, P. M. (2012). Analysis of Nonmodifiable Risk Factors for Intracranial Aneurysm Rupture in a Large, Retrospective Cohort. *Neurosurgery*, 70(3), 693–701. <https://doi.org/10.1227/neu.0b013e3182354d68>
- Cebal, J. R., Mut, F., Weir, J., & Putman, C. M. (2011). Association of hemodynamic characteristics and cerebral aneurysm rupture. *American Journal of Neuroradiology*, 32(2), 264–270. <https://doi.org/10.3174/ajnr.A2274>
- Chiu, J. J., & Chien, S. (2011). Effects of disturbed flow on vascular endothelium: Pathophysiological basis and clinical perspectives. *Physiological Reviews*, 91(1), 327–387. <https://doi.org/10.1152/physrev.00047.2009>
- Doutel, E., Carneiro, J., Oliveira, M. S. N., Campos, J. B. L. M., & Miranda, J. M. (2015). Fabrication of 3d milli-scale channels for hemodynamic studies. *Journal of Mechanics in Medicine and Biology*, 15(1), 1–21. <https://doi.org/10.1142/S0219519415500049>
- Hopkins, L. M., Kelly, J. T., Wexler, A. S., & Prasad, A. K. (2000). Particle image velocimetry measurements in complex geometries. *Experiments in Fluids*, 29(1), 91–95. <https://doi.org/10.1007/s003480050430>
- Parlea, L., Fahrig, R., Holdsworth, D. W., & Lownie, S. P. (1999). An Analysis of the Geometry of Saccular Intracranial Aneurysms. *AJNR Am J Neuroradiol*, 1079–1089.
- Philip, N. T., Bolem, S., Sudhir, B. J., & Patnaik, B. S. V. (2022). Hemodynamics and bio-mechanics of morphologically distinct saccular intracranial aneurysms at bifurcations: Idealised vs Patient-specific geometries. *Computer Methods and Programs in Biomedicine*, 227, 107237. <https://doi.org/10.1016/j.cmpb.2022.107237>
- Rodriguez-Régent, C., Edjlali-Goujon, M., Trystram, D., Boulouis, G., Ben Hassen, W., Godon-Hardy, S., Nataf, F., MacHet, A., Legrand, L., Ladoux, A., Mellerio, C., Souillard-Scemama, R., Oppenheim, C., Meder, J. F., & Naggara, O. (2014). Non-invasive diagnosis of

- intracranial aneurysms. *Diagnostic and Interventional Imaging*, 95(12), 1163–1174. <https://doi.org/10.1016/j.diii.2014.10.005>
- Roloff, C., Stucht, D., Beuing, O., & Berg, P. (2018). *Comparison of intracranial aneurysm flow quantification techniques: standard PIV vs stereoscopic PIV vs tomographic PIV vs phase-contrast MRI vs CFD*. 1–8. <https://doi.org/10.1136/neurintsurg-2018-013921>
- Saqr, K. M., Rashad, S., Tupin, S., Niizuma, K., Hassan, T., Tominaga, T., & Ohta, M. (2019). What does computational fluid dynamics tell us about intracranial aneurysms? A meta-analysis and critical review. *Journal of Cerebral Blood Flow and Metabolism*. <https://doi.org/10.1177/0271678X19854640>
- Souza, A., Souza, M. S., Pinho, D., Agujetas, R., Ferrera, C., Lima, R., Puga, H., & Ribeiro, J. (2020). 3D manufacturing of intracranial aneurysm biomodels for flow visualizations: Low cost fabrication processes. *Mechanics Research Communications*, 107, 103535. <https://doi.org/10.1016/j.mechrescom.2020.103535>
- Szajer, J., & Ho-Shon, K. (2018). A comparison of 4D flow MRI-derived wall shear stress with computational fluid dynamics methods for intracranial aneurysms and carotid bifurcations — A review. *Magnetic Resonance Imaging*, 48, 62–69. <https://doi.org/10.1016/j.mri.2017.12.005>
- Tromp, G., Weinsheimer, S., Ronkainen, A., & Kuivaniemi, H. (2014). Molecular basis and genetic predisposition to intracranial aneurysm. *Annals of Medicine*, 46(8), 597–606. <https://doi.org/10.3109/07853890.2014.949299>
- Yamaguchi, R., Tanaka, G., Shafii, N. S., Osman, K., Shimizu, Y., Saqr, K. M., & Ohta, M. (2022). Characteristic effect of wall elasticity on flow instability and wall shear stress of a full-scale, patient-specific aneurysm model in the middle cerebral artery: An experimental approach. *Journal of Applied Physics*, 131(18). <https://doi.org/10.1063/5.0085417>
- Yu, P., & Durgesh, V. (2022). Experimental study of flow structure impact on the fluid parameters in saccular aneurysm models. *Experimental Thermal and Fluid Science*, 138(July 2021), 110675. <https://doi.org/10.1016/j.expthermflusci.2022.110675>